

2

AD-A264 755

NTATION PAGE

Form Approved
OMB No. 0704-0188



Not to exceed 1 hour per volume, including the time for reviewing instructions, searching existing data sources, reviewing the collection of information. Send comments regarding this burden estimate or any other aspect of this burden to Washington Headquarters Services, Directorate for Information Operations and Reports, 1215 Jefferson Office of Management and Budget, Paperwork Reduction Project (0704-0188), Washington, DC 20503.

1. REPORT DATE: FINAL
2. REPORT TYPE AND DATES COVERED: FINAL 15 Sep 91 TO 14 Sep 92

4. TITLE AND SUBTITLE
Atomic layer epitaxy of semiconductor heterostructures

5. FUNDING NUMBERS
AFOSR-91-0422

6. AUTHOR(S)
Professor Salah Bedair

DTIC
ELECTE
MAY 14 1993
S C D

7. PERFORMING ORGANIZATION NAME(S) AND ADDRESS(ES)
Dept of Electrical Engineering
North Carolina State Univ
Raleigh, NC 279695-7911

8. PERFORMING ORGANIZATION REPORT NUMBER
AFOSR-

9. SPONSORING/MONITORING AGENCY NAME(S) AND ADDRESS(ES)
AFOSR/NE
Bldg 410
Bolling AFB Washington, DC 20332-6448
LTC Gernot Pomrenke

10. SPONSORING/MONITORING AGENCY REPORT NUMBER
2305/B1

11. SUPPLEMENTARY NOTES

93-10699



12. DISTRIBUTION/AVAILABILITY STATEMENT
APPROVED FOR PUBLIC RELEASE: DISTRIBUTION IS UNLIMITED
00 3 12 142

13. ABSTRACT (Maximum 200 words)
AlGaP and GaP films were deposited on the (100) Si substrates by Atomic Layer Epitaxy (ALE) in the temperature range between 450 and 600°C. Under optimum growth conditions, the growth of GaP and AlGaP was observed to proceed in a two-dimensional (2-D) fashion in the initial growth stages. These ALE-grown films have better surface morphology when compared with the corresponding MOCVD-grown films. With an AlGaP buffer layer grown on Si, the subsequent growth of GaAs on the AlGaP-coated Si substrates tends to proceed 2-D growth. This avoids island growth and the two-step growth process currently used.

14. SUBJECT TERMS

15. NUMBER OF PAGES
16. PRICE CODE

17. SECURITY CLASSIFICATION OF REPORT
UNCLASSIFIED

18. SECURITY CLASSIFICATION OF THIS PAGE
UNCLASSIFIED

19. SECURITY CLASSIFICATION OF ABSTRACT
UNCLASSIFIED

20. LIMITATION OF ABSTRACT
UNLIMITED

FINAL REPORT

ATOMIC LAYER EPITAXY OF SEMICONDUCTOR HETEROSTRUCTURES

U.S. AIR FORCE: AFOSR - 91 - 0422

PREPARED BY

**S.M. BEDAIR
DEPARTMENT OF ELECTRICAL AND COMPUTER ENGINEERING
NORTH CAROLINA STATE UNIVERSITY
RALEIGH, NC 27695-7911**

NOVEMBER 1992

| | |
|--------------------|-------------------------------------|
| Accession For | |
| NTIS CRA&I | <input checked="" type="checkbox"/> |
| DTIC TAB | <input type="checkbox"/> |
| Unannounced | <input type="checkbox"/> |
| Justification | |
| By | |
| Distribution/ | |
| Availability Codes | |
| Dist | Avail and/or Special |
| A-1 | |

Project Summary and Achievements

The objective of this project is the use of Atomic Layer Epitaxy for the low temperature and 2-D growth of GaAs, GaP on silicon substrates and also highly strained films of GaP on GaAs. The major achievements can be summarized as follows:

1. Low Temperature Growth of AlGaP and GaP on Si Substrates by Atomic Layer Epitaxy

AlGaP and GaP films were deposited on the (100) Si substrates by Atomic Layer Epitaxy (ALE) in the temperature range between 450 and 600°C. Under optimum growth conditions, the growth of GaP and AlGaP was observed to proceed in a two-dimensional (2-D) fashion in the initial growth stages. These ALE-grown films have better surface morphology when compared with the corresponding MOCVD-grown films. With an AlGaP buffer layer grown on Si, the subsequent growth of GaAs on the AlGaP-coated Si substrates tends to proceed 2-D growth. This avoids island growth and the two-step growth process currently used.

2. Properties of Highly Strained GaP and GaP/GaAs/GaP Quantum Wells Grown on GaAs Substrates by Atomic Layer Epitaxy

Atomic Layer Epitaxy (ALE) has been employed for the growth of highly strained (3.6%) GaP films and GaP/GaAs/GaP single quantum wells on (100) GaAs substrates at 500°C. Misfit dislocation formation in GaP was observed by Scanning Transmission Electron Microscopy (STEM) and chemical delineation of dislocations. The onset of dislocations in the GaP layers was also determined by the onset of degradation in electrical properties (breakdown voltage and reverse current) of GaP/GaAs Schottky diodes and in low temperature photoluminescence (FWHM and intensity) of GaP/GaAs/GaP single quantum wells. All techniques experimentally indicate a critical layer thickness (CLT) greater than 60 Å. This value is several times larger than the theoretical value ($h_c < 20 \text{ \AA}$) predicted by the force balance model. This result may be related to the low growth temperature and the two dimensional (2-D) nature of the ALE growth process.

LOW TEMPERATURE GROWTH OF AlGaP AND GaP ON Si SUBSTRATES BY ATOMIC LAYER EPITAXY

J.R. Gong, S. Nakamura,** M. Leonard, S.M. Bedair,* and N.A. El-Masry

Department of Materials Science and Engineering, North Carolina State University, Raleigh, N.C. 27695-7916

* Department of Electrical and Computer Engineering, North Carolina State University, Raleigh, N.C. 27695-7911

** On leave from Semiconductor Division, Sumitomo Metal Inc., Japan

ABSTRACT

AlGaP and GaP films were deposited on the (100) Si substrates by Atomic Layer Epitaxy (ALE) in the temperature range between 450 and 600 °C. Under optimum growth conditions, the growth of GaP and AlGaP was observed to proceed in a two-dimensional (2-D) fashion in the initial growth stages. These ALE-grown films have better surface morphology when compared with the corresponding MOCVD-grown films. With an AlGaP buffer layer grown on Si, the subsequent growth of GaAs on the AlGaP-coated Si substrates tends to proceed 2-D growth. This avoids island growth and the two-step growth process currently used.

I. INTRODUCTION

Recent advances in the III-V on Si heteroepitaxy have received great attention due to the potential advantages of the monolithic integration of III-V optoelectronic devices with Si integrated circuits. Among the III-V compound semiconductors, GaP is of particular interest for this integration with Si, primarily, because of its small lattice-mismatch (0.37% at room temperature) with Si. Also, GaP has been utilized as the material for light-emitting diodes (LED's).¹ With proper doping, various visible emissions were attainable in GaP LED's. Therefore, from the application point of view, the possibility of growing good quality GaP epitaxial films on the (100) Si substrates is very attractive. Several approaches have been used to grow GaP on Si;^{2,3} however, most of the results were not encouraging. The major problem of the growth of GaP on Si, like GaAs on Si, has been addressed to be the three-dimensional (3-D) growth mode in the early stages of growth. For the MOCVD growth, it has been reported that GaP films were polycrystalline in the temperature range of 500 ~ 800 °C⁴. To avoid island growth, various efforts have recently been proposed such as the incorporation of high Al content in the grown films⁵ and the initiation of As-Si bonding⁶ prior to growth in order to strengthen the bonding between the grown film and substrate. However, to achieve 2 D-like growth, the AlGaP and GaP films have to be prepared at high temperature (~ 900 °C), and the V/III ratio needs to be very high.⁷ Such high temperature and V/III ratio may not be adequate for the growth of GaP on Si because of interdiffusion problems.

Atomic layer epitaxy (ALE), as a growth technique, has demonstrated its feasibility for the growth of various semiconductor materials. The advantages of this technique include low temperature growth, migration enhancement of the adsorbed species on the grown surface,

precision in film thickness control, and so forth. Low temperature growth helps to minimize the interdiffusion between the grown film and substrate, which is prominent for high temperature growth. The increment in the mobilities of the adatoms on the grown surface is helpful for achieving better material quality. In this paper, we will present the results of the ALE growth of AlGaP and GaP films on Si, as well as the ALE growth of GaAs on the AlGaP-coated Si substrates.

II. EXPERIMENTAL PROCEDURE

The growth of AlGaP and GaP films on Si substrates was carried out in an atmospheric pressure ALE reactor. The graphite susceptor was specially designed for the substrate-rotating ALE growth approach established at North Carolina State University since 1985.⁸ Trimethylgallium (TMG) and trimethylaluminum (TMA) were used as the sources for group III elements with bubbler temperature kept at -10 and 17 °C, respectively. PH₃ and AsH₃ (10% in H₂), purified by a reactive resin (millipore), were utilized as the group V source materials. The vicinal (100) Si substrates (3° tilted about the <011> axis) were solvent-cleaned, dipped in a 5% HF solution, followed by boiling in a solution of HCl:H₂O₂:H₂O (1:1:4) for 3 minutes before loading. Prior to growth, the Si substrate was heated to 1040 °C under an H₂ ambient for 20 minutes. The substrate was, then, cooled to the growth temperature with PH₃ being introduced to the substrate surface at 900 °C. The ALE growth of AlGaP proceeds by alternatively exposing the Si substrate to the TMG/TMA fluxes in the column III and the PH₃ flux in the column V. A typical ALE growth cycle takes 5 seconds with an exposure time of 0.6 seconds for each column and a pause length of 1.9 seconds between each exposure. The ALE-grown films were

characterized by ellipsometric measurements for revealing thickness and refractive index uniformity. Transmission electron microscopy (TEM) was employed for structural defect analyses. Surface morphology of the grown layers was examined by scanning electron microscopy (SEM).

III. RESULTS AND DISCUSSION

The ALE-grown GaP films were observed to completely cover the Si substrate surface in the early stages of growth, in the temperature range of 450 ~ 600 °C. Figure 1(a) shows a cross-sectional TEM micrograph of a thin GaP (~ 300 Å) layer grown at 600 °C. The plan-view diffraction pattern of this thin GaP layer (Figure 1(b)) illustrates the single crystal nature of the GaP layer. However, when the growth temperature is low enough (≤ 500 °C), as the GaP layer thickness reaches a certain value (for example, ~ 300 Å at 500 °C), the film becomes polycrystalline. Similar tendency was also observed in the case of AlGaP films grown by ALE. It was found that single crystal AlGaP and GaP layers could be prepared by ALE at growth temperatures of 550 and 600 °C, respectively. For comparison, we also performed the MOCVD growth of GaP on Si using the same susceptor, reactor, and flow rates of the reactants. Our result of MOCVD growth of GaP films on Si is consistent with the previous results. The MOCVD-grown GaP films are polycrystalline at 600 °C as revealed in the SEM micrograph (Figure 2(a)). In contrast to the rough surface morphology of the MOCVD-grown films, the GaP films prepared by ALE growth at the same temperature show smooth surface morphology (Figure 2(b)). It has previously been reported⁴ that the MOCVD growth of single crystal GaP films on Si using TMG and PH₃ is not achievable at a constant temperature of 800 °C or less.

For preparing single crystal GaP layer on Si, Olson et al.⁴ have to resort to a two-step growth process where a thin polycrystalline GaP film was first deposited at low temperatures (≤ 500 °C) with a subsequent growth of GaP layer at high temperatures (≥ 750 °C). Although single crystal GaP films have been reported to achieve by high temperature (~ 900 °C) MOCVD growth, the initial growth of GaP is observed to be in the form of separate islands unless the V/III ratio is increased to very high values (≥ 600).⁷

The poor surface morphology of the MOCVD-grown GaP films is due to the polycrystalline nature of the films because of the insufficient migration of the GaP molecules (or aggregates) at low temperatures.⁷ It has been reported that the group III adatoms on the grown surface have higher migration velocities in the absence of hydrides of group V element.⁹ Thus, the better surface morphology in the ALE-grown GaP films could be the consequence of the enhancement of the surface mobilities of the adatoms. Since surface migration is a thermally activated process, growth temperature plays an important role in the material quality of the grown films. For the temperature range of current investigations, the higher the growth temperature is, the better the material quality will be. At low temperatures, in particular, the film quality may not be good enough during the early growth stages because of insufficient migration, the material quality of the subsequently grown film is expected to be poor. Thus, it is believed that the polycrystalline nature of the ALE-grown GaP and AlGaP films, when they were grown on Si at 500 °C (or less), is the result of insufficient migration of the adatoms.

Figure 3 shows a plot of the growth rate of AlGaP films versus the (TMA+TMG) fluxes at 550 °C with a constant column III gas phase composition ($\text{TMA}/[\text{TMA}+\text{TMG}]$) of 0.04. The thickness measurement is based on the cross-sectional TEM studies on the AlGaP films with

thicknesses of about 2000 Å using (200) two-beam condition. It appears that the growth rate is not dependent upon the (TMA+TMG) fluxes over a self-limiting window where the growth rate saturates slightly above one monolayer per ALE cycle. It is not clear at this point why the growth rate saturates slightly above one monolayer per ALE cycle. One possibility could be due to high V/III ratio which may cause cross-diffusion of PH_3 toward column III. More work is necessary to elucidate this point.

Both film thickness and refractive index are uniform in all the ALE-grown AlGaP samples. Figure 4 shows a typical thickness and refractive index uniformity across a distance along the direction of the rotation tangent. The values of thickness and refractive index were obtained by ellipsometric measurements. As shown in Figure 4, the variations in thickness and refractive index, across 9 mm distance, were 0.2% and 0.6%, respectively. A similar result has been reported in our recent studies on the ALE growth of AlGaAs¹⁰ where the composition and thickness uniformity is greatly improved in the ALE growth when compared with the results of MOCVD growth. It is generally believed that a minimization in thickness and composition variations on the grown films is energetically favorable in terms of surface and chemical free energies. Accordingly, the achievement of good uniformity in film thickness and composition distributions is also believed to be facilitated by the migration enhancement of the adsorbed species on the grown surface.

A reduction in the exposure time and the pause time between exposures for each growth cycle tends to promote 2-D growth of AlGaP on the (100) Si substrate in the early growth stages. Figure 5 shows a cross-sectional TEM micrograph (with an inset of plan-view diffraction pattern) of a 300 Å AlGaP film grown on Si at 500 °C by ALE. In this case, the exposure time

to each column and the pause time between exposures were 0.24 sec and 0.76 sec, respectively. It is apparent that the AlGaP film thickness is very uniform in the early stages of the ALE growth. The fact that a reduction in exposure time and pause time during the ALE growth of AlGaP is in favor of 2-D deposition in the early growth stages can be interpreted as follows. During the ALE growth, the surface diffusion lengths of the adsorbed species may primarily be controlled by substrate temperature. However, the diffusion lengths of the adsorbed species can also be affected by the deposition rate when the substrate temperature is low enough. Since the temperature range of current ALE growth of AlGaP on Si is far below the melting point of AlGaP (> 1400 °C), the effect of thermal energy on the surface mobilities of the adsorbed species is possibly less significant. It is reasonable to believe that a further decrement in the surface diffusion lengths may become prominent by reducing the exposure time and pause time of each ALE cycle. Therefore, this decrement in the surface diffusion lengths is helpful in promoting 2-D deposition in the early growth stages. A similar argument has recently been addressed in the case of high temperature MOCVD growth of GaP on Si with extremely high V/III ratios.¹¹ In this case, 2-D growth is attributed to the large amount of adsorbed phosphorus which is effective in capturing the migrating species.

AlGaP has recently been proposed as an intermediate layer for the growth of GaAs on Si, primarily because that the AlGaP layer allows to isolate the polar-on-nonpolar and lattice-mismatch problems in the heteroepitaxy of GaAs on Si substrates. However, previous results¹² show that GaAs tends to form island growth on the AlGaP-coated Si substrates even though the AlGaP films can be prepared two-dimensionally at 900 °C by MOCVD growth. As a consequence, alternative approach by using other Al-containing intermediate layer such as

AlGaAs films was proposed to explore the possible 2-D growth of GaAs on Si.¹² In this study, we also performed the ALE growth of GaAs on the AlGaP-coated Si substrate at 500 °C. Figures 6(a) and (b) illustrate the cross-sectional and plan-view TEM micrographs of a thin GaAs layer (~ 600 Å) grown by ALE on an AlGaP-coated Si substrate. In this case the growth temperature is 500 °C, and the AlGaP layer thickness is ~ 150 Å. One can clearly see in Figure 6(a) that the planar GaAs layer completely covers the AlGaP-coated Si substrate. The plan-view micrograph (Figure 6(b)) shows parallel Moiré fringes due to the double diffractions from AlGaP and GaAs layers. The measured value of the Moiré fringe spacings is about 50 Å, which is in good agreement with the calculated value of 56 Å. It appears that both GaAs and AlGaP films are single crystal.

The major defects observed in all the ALE-grown GaP, AlGaP, and GaAs films were the planar defects such as stacking faults and microtwins, as well as threading dislocations. These defects have also been reported in the case of low temperature MOCVD growth. The cause of the planar defects is still controversial. Several groups^{13,14} believe that these defects are caused by the mismatch of lattice constants or thermal expansion coefficients between the GaP films and the Si substrates. Others,¹⁵ on the other hand, believe that the formation of planar defects in the GaP films grown on Si is a consequence of the stacking errors of the adsorbed species on the closed-packed planes during the early stages of nucleation and growth rather than the result of strain relief. The reason for the formation of threading dislocations in the AlGaP and GaP films grown on Si can partially be explained by the strain relaxation in the grown films. However, it can not explain why the threading dislocations rather than the misfit dislocations are formed. It has been reported that,¹⁶ for the growth of Si layers on the (100) GaP substrates, no defect was

observed when the Si layer thickness is less than 1000 Å. Even when the Si layer thickness is higher than this critical value, the defects observed are mainly misfit dislocations. Since the Si on GaP growth is the counterpart of the GaP on Si growth, the effect due to lattice and thermal mismatches is presumably similar. Thus, the formation of threading dislocations in the GaP and AlGaP layers could possibly be related to the formation of surface defects such as SiC after the annealing at 1040 °C, which is not high enough to completely eliminate the SiC centers¹⁷ on the Si surface. More work is necessary for a complete picture of the cause of dislocation generation.

In conclusion, the ALE growth of GaP and AlGaP films on the (100) Si substrates was reported. The self-limiting growth behavior of the AlGaP films on the Si substrates was identified. The ALE-grown films showed better surface morphology than the MOCVD films. Very good composition and thickness uniformity across the ALE-grown AlGaP films was achieved. The initial growth of AlGaP films can proceed in a 2-D fashion when the exposure time and the pause time of each ALE growth cycle are optimized. Planar GaAs layers can also be prepared on the AlGaP-coated Si substrates. The implementation of ALE technology is potentially applicable for the growth of GaP and AlGaP films on Si, as well as GaAs on AlGaP-coated Si.

This work is supported by SDIO/ONR, National Science Foundation, and Solar Energy Research Institute.

REFERENCES:

1. R.N. Bhargava, IEE Trans. Electron. Dev. ED-22, 691 (1975).
2. L. Samuelson, P. Omling, and H.G. Grimmeiss, J. Crystal Growth 68, 340 (1984).
3. H. Kawanami, T. Sakamoto, T. Takahashi, E. Suzuki, and K. Nagai, Jpn. J. Appl. Phys. 21, L68 (1982).
4. J.M. Olson, M.M. Al-Jassim, A. Kibbler, and K.M. Jones, J. Crystal Growth 77, 515 (1986).
5. T. George, E.R. Weber, S. Nozaki, A.T. Wu, N. Noto, and M. Umeno, J. Appl. Phys. 67, 2441 (1990).
6. Y. Kohama, K. Uchida, T. Soga, T. Jimbo, and M. Umeno, Appl. Phys. Lett. 53, 862 (1988).
7. M. Imaizumi, T. Saka, T. Jimbo, T. Soga, and M. Umeno, Jpn. J. Appl. Phys. 30, 451 (1991).
8. M.A. Tischler and S.M. Bedair, Appl. Phys. Lett. 48, 1961 (1986).
9. T.H. Chin, Appl. Phys. Lett. 55, 1244 (1989).
10. J.R. Gong, D. Jung, N.A. El-Masry, and S.M. Bedair, Appl. Phys. Lett. 57, 400 (1990).
11. T. Soga, T. George, T. Suzuki, T. Jimbo, and M. Umeno, and E.R. Weber, Appl. Phys. Lett. 58, 2108 (1991).
12. T. Soga, T. George, T. Jimbo, M. Umeno, and E.R. Weber, Appl. Phys. Lett. 58, 1170 (1991).
13. M.M. Al-Jassim, J.M. Olson, and K.M. Jones, Mater. Res. Soc. Symp. Proc. 62, 49 (1986).

14. D.K. Biegelsen, F.A. Ponce, A.J. Smith, and J.C. Tramontana, *J. Appl. Phys.* 61, 1856 (1987).
15. F. Ernst and P. Pirouz, *J. Appl. Phys.* 64, 4526 (1988).
16. P.M.J. Marée, J.C. Barbour, J.F. van der Veen, K.L. Kavanagh, C.W.T. Bulle-Lieuwma, and M.P.A. Vieggers, *J. Appl. Phys.* 62, 4413 (1987).
17. D. Dijkkamp, A.J. Hoeven, E.J. van Loenen, J.M. Lenssinck, and J. Dieleman, *Appl. Phys. Lett.* 56, 39 (1990).

FIGURE CAPTIONS:

1. TEM micrographs of a 300 Å GaP layer grown on Si by ALE at 600 °C. (a) cross-sectional view image. (b) plan-view diffraction pattern.

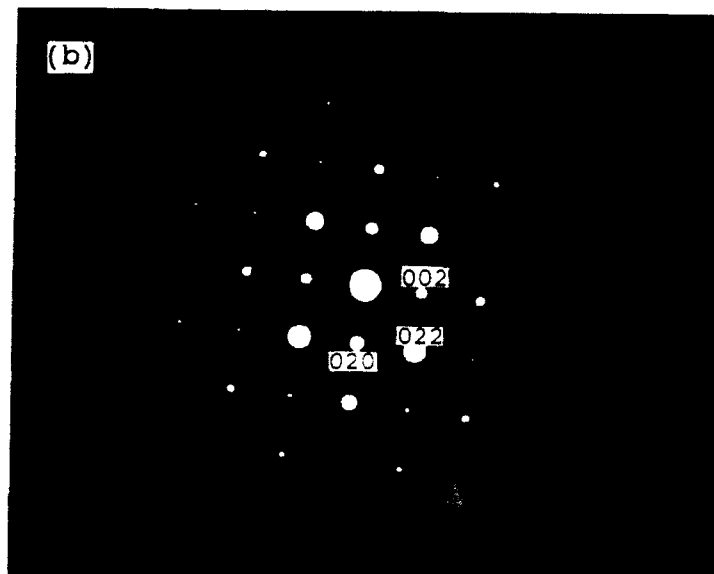
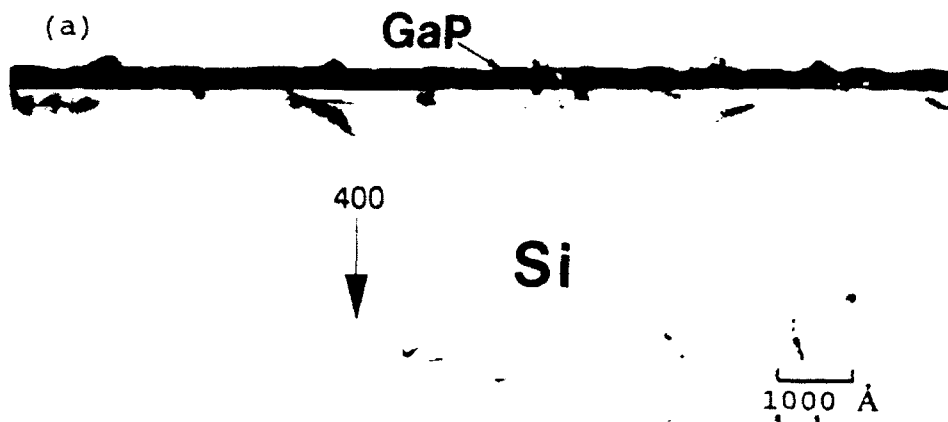
2. (a) SEM micrograph of the surface morphology of the GaP film grown at 600 °C by MOCVD.
(b) SEM micrograph of the surface morphology of the GaP film grown at 600 °C by ALE.

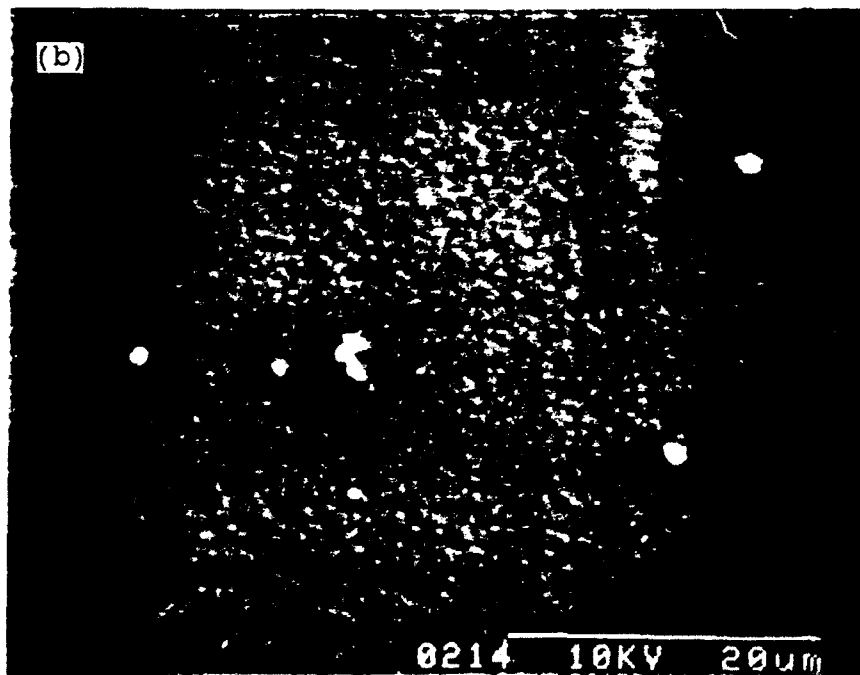
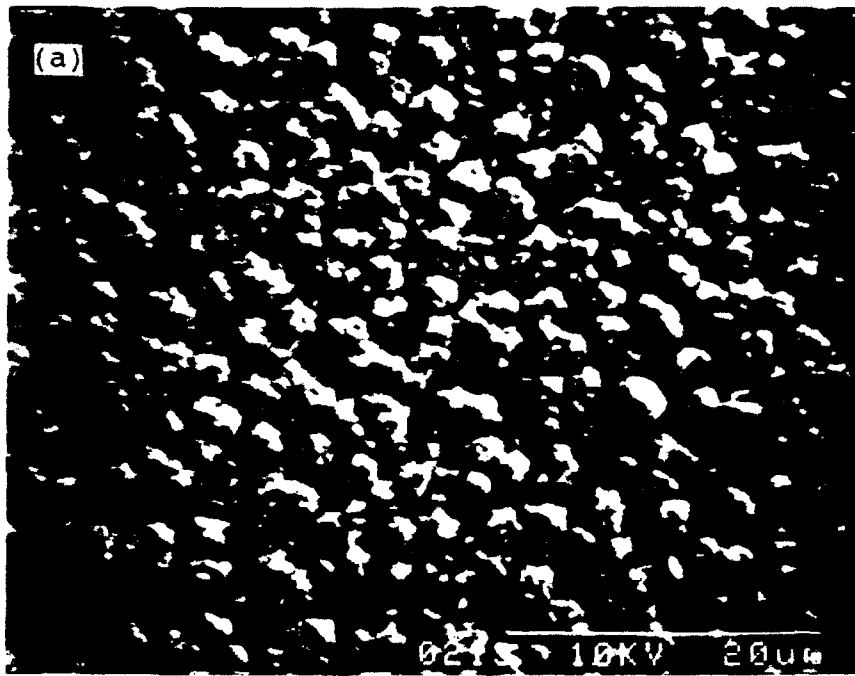
3. AlGaP film thickness per ALE cycle vs. (TMA + TMG) flux at 550 °C.

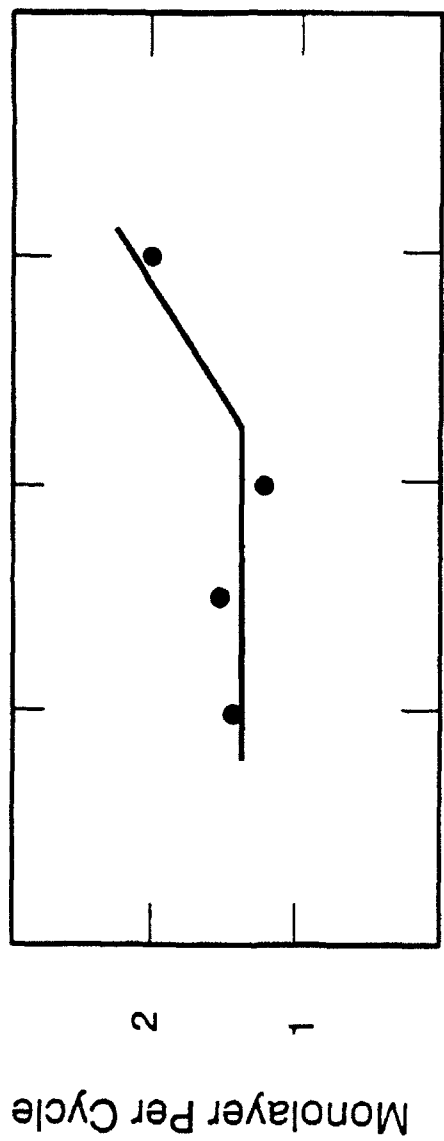
4. Thickness and refractive index uniformity of a typical AlGaP film grown on the Si substrate.

5. Cross-sectional TEM micrograph of a 300 Å AlGaP film grown on Si at 500 °C with an inset of the corresponding plan-view diffraction pattern.

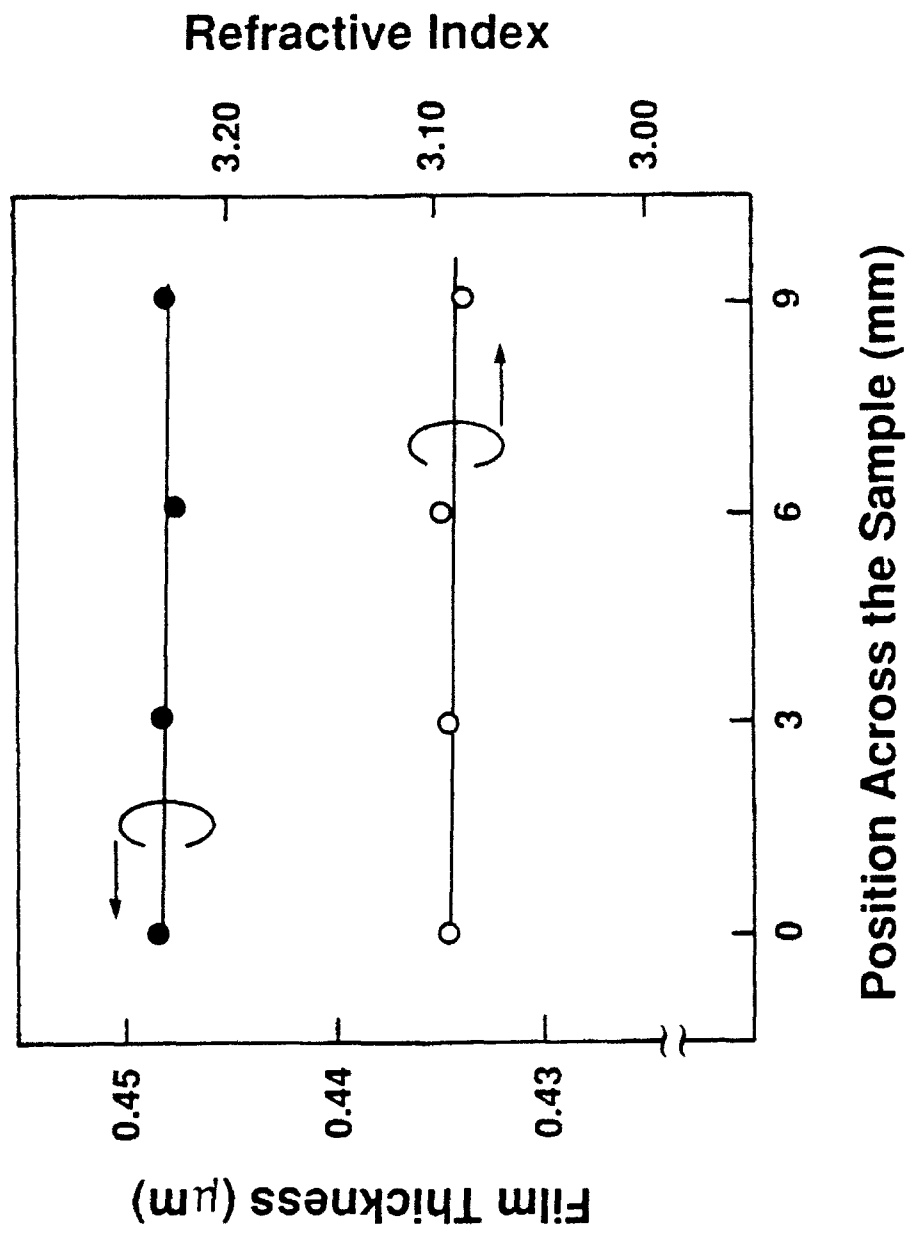
6. TEM micrographs of a 600 Å GaAs layer grown on an AlGaP-coated Si substrate.
(a) cross-sectional view. (b) plan-view.

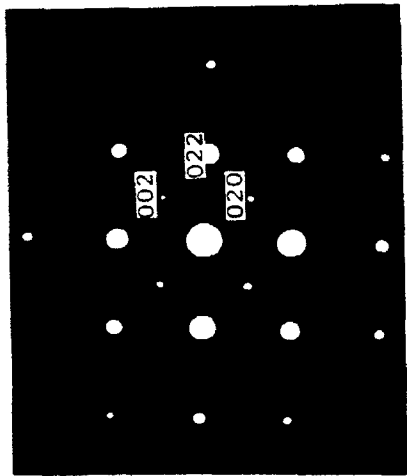
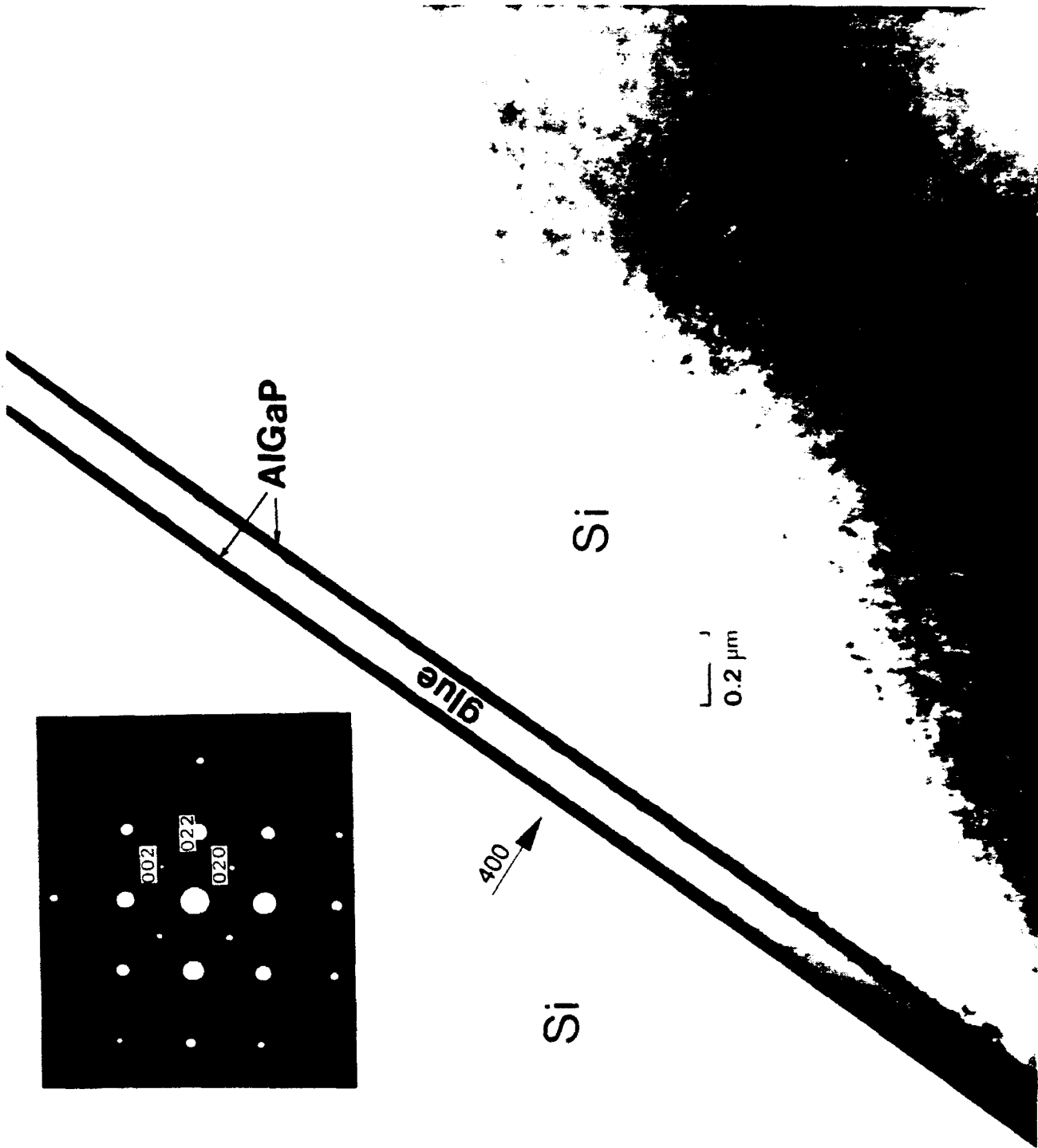


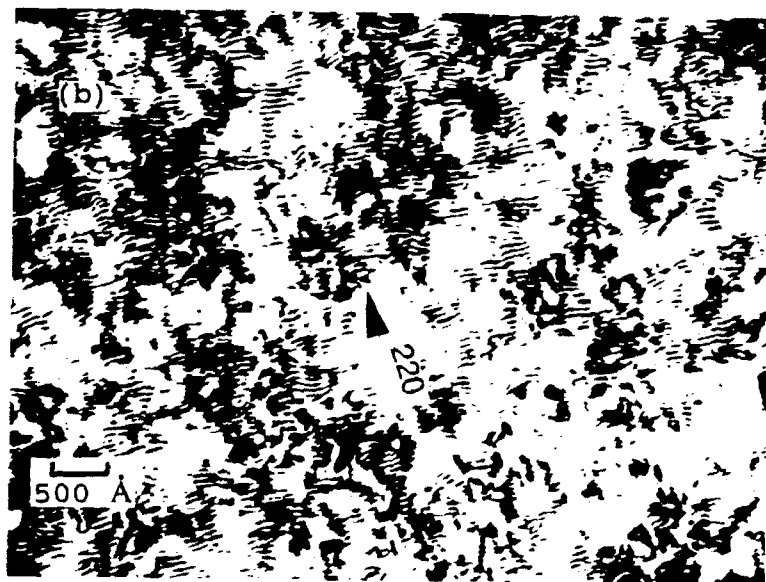
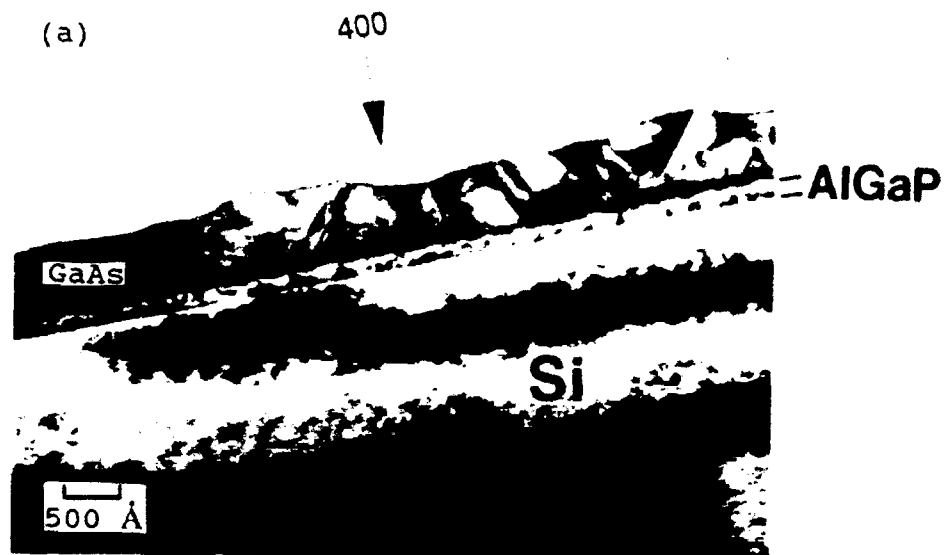




TMGa + TMAI (μmole/cycle)







**PROPERTIES OF HIGHLY STRAINED GaP and
GaP/GaAs/GaP QUANTUM WELLS GROWN ON GaAs
SUBSTRATES BY ATOMIC LAYER EPITAXY**

C.A.Parker, J.R.Gong, D.Jung, F.Huga^{a1}, N.A.El-Masry, and S.M.Bedair

Department of Electrical and Computer Engineering

North Carolina State University

Raleigh, North Carolina 27695-7911

^{a1}On leave from NTT LSI Laboratories, 3-1, Morinosato

Wakamiya, Atsugi-shi, Kanagawa, 243-01 Japan.

To be submitted.

Abstract

Atomic layer epitaxy (ALE) has been employed for the growth of highly strained (3.6%) GaP films and GaP/GaAs/GaP single quantum wells on (100) GaAs substrates at 500°C. Misfit dislocation formation in GaP was observed by Scanning Transmission Electron Microscopy (STEM) and chemical delineation of dislocations. The onset of dislocations in the GaP layers was also determined by the onset of degradation in electrical properties (breakdown voltage and reverse current) of GaP/GaAs Schottky diodes and in low temperature photoluminescence (FWHM and intensity) of GaP/GaAs/GaP single quantum wells. All techniques experimentally indicate a critical layer thickness (CLT) greater than 60 Å. This value is several times larger than the theoretical value ($h_c < 20$ Å) predicted by the force balance model. This result may be related to the low growth temperature and the two dimensional (2-D) nature of the ALE growth process.

Introduction

Due to the tailorable nature in the optical and electrical properties, pseudomorphic strained layer epitaxy has attracted much attention in recent years as a source for alternative heterostructure materials. Several systems such as GaInAs/InP^{1,2}, GeSi/Si^{3,4}, InGaAs/GaAs^{5,9}, GaAsP/GaP¹⁰, and GaAsP/GaAs^{11,12} have already been investigated intensively from both material and device aspects. In strained layer epitaxy, layers are grown lattice mismatched to the substrate where pseudomorphic growth is supported for layers less than the critical layer thickness (CLT)¹³. When the layer thickness exceeds the CLT, the mismatch is accommodated by both elastic strains and generations of misfit dislocations¹³. These misfit dislocations degrade the structural, optical and electrical properties of materials¹³. Therefore, it is very important to determine clearly the CLT value in strained layer systems. Large lattice-mismatch strained-layer systems that have very thin critical thicknesses require precise control of deposition rate and thickness uniformity. Atomic layer epitaxy (ALE) is a suitable candidate for growth of ultra-thin highly strained pseudomorphic layers due to its unique self-limiting mechanism.

The highly strained GaP/GaAs system grown on GaAs substrates with a mismatch of 3.6% can utilize GaP as a wide bandgap (2.26 eV at room temperature) alternative to the more commonly used semiconductor compounds with Al as a group III species. However,

the thickness of a single dislocation-free GaP layer grown on a GaAs substrate is limited to a CLT of approximately 16 Å as predicted by the theoretical force balance model of Matthews and Blakeslee¹². If thicker barrier layers are required to provide better confinement of carriers and prevent tunneling, the thickness of the high bandgap GaP layer must exceed the theoretical CLT. We report in this paper that the monolayer-by-monolayer and low temperature ALE growth can achieve GaP with layer thickness greater than the theoretical CLT that can be suitable for device potential applications. A single GaP overgrown layer and GaP/GaAs/GaP single quantum well structures grown on GaAs will be studied to determine the CLT in ALE grown layers.

Growth

The ALE growth of GaP and GaAs was achieved in an atmospheric-pressure quartz reactor with a specially designed graphite susceptor which has been described in detail elsewhere¹⁴. TMGa was employed as the source of column III metal with bubbler temperature kept at -10 °C. The PH₃ and AsH₃ were utilized as column V source materials. The ALE growth for each layer entailed alternatively exposing the substrate to column III and column V streams of organometallic and hydride precursors. A constant 4 slm hydrogen flow was injected into the reactor by a central inlet tube during the growth.

All GaP layers in this study were grown by ALE at 500 °C. To prevent the growth of the ternary compound GaAsP and ensure interfacial abruptness after growth of a GaAs layer, the GaAs

sample was first positioned under the AsH₃ flux for 15 seconds; then the AsH₃ flux was turned off while the PH₃ flux was turned on. Prior to growth of the GaP layer, the sample was held stationary under the PH₃ flux for several seconds with a high hydrogen flow at low temperature (500 °C) to ensure removal of the AsH₃ gas from the reactor. An inversion of this technique was employed when switching from PH₃ to AsH₃ before growing GaAs on GaP in the strained quantum well studies.

The substrates used in the GaP/GaAs Schottky diode studies were semi-insulating (100) GaAs wafers. First, a 2000 Å undoped GaAs buffer layer was grown at 650°C utilizing a conventional MOCVD approach where the substrate is stationary and exposed to the TMGa and AsH₃ fluxes simultaneously. The buffer layer was followed by a 2000 Å Si-doped ($3 \times 10^{17} \text{ cm}^{-3}$) GaAs layer grown by ALE at 550°C. Finally, an ALE GaP layer was grown at 500°C. The planar Schottky device was fabricated first by evaporating a AuGe/Au (350 Å/1500 Å) Ohmic contact with an E-beam evaporator on a photoresist patterned surface followed by an anneal step at 425°C for 30 seconds in N₂. Next, a Schottky Ti/Au (600 Å/1500 Å) contact by E-beam evaporation was fabricated with a diode area 280 μm x 280 μm.

The characterization techniques used to determine the CLT of GaP on (100) GaAs were Transmission Electron Microscopy (TEM), chemical etch delineation of dislocations, electrical characteristics of GaP/GaAs Schottky diodes, and low temperature photoluminescence spectroscopy of strained GaP/GaAs/GaP single quantum wells.

Results and Discussion

TEM was used to view dislocation formation in GaP layers. Figures 1(a)-(c) show the plan-view TEM micrographs of the GaP layers on GaAs characterized by a Hitachi 800 Transmission Electron Microscope operating at 200 KV. The thickness of these GaP layers are 60, 80, and 200 Å, respectively, as determined from the ALE number of cycles. It appears a dislocation density was observed when the thickness of GaP layers increased from 60 to 80 Å. As revealed in Figure 1(c), most of the dislocation lines are of the misfit type running along [110] and [1-10] directions when the GaP layer thickness reaches approximately 200 Å. The rapid increase in dislocation density is an indication of strain relaxation by dislocation formation due to the very large lattice mismatch. From the dislocation onset, TEM suggest a CLT occurring between 60 and 80 Å.

Delineation of dislocations at the interface surface by chemical etching was also applied to study dislocation formations in the GaP layer grown on GaAs. The GaP layer was first removed by HCl followed by $H_3PO_4 : H_2O_2 : H_2O$ (3:1:50) to remove the GaAs epilayer. Possibly due to cluster 3-D nucleation, discussed later in detail, in GaP layers exceeding a critical layer thickness, delineation of the 3-D clusters and associated dislocations in these GaP layers can be seen. This dislocation delineation shown in Figure 2(a) and 2(b) are photographs taken from an optical microscope of the 60 Å GaP and 140 Å GaP samples after the mesa etch. A photograph of the 100 Å GaP sample was the same as the 60 Å GaP sample. This

technique is clearly not as sensitive as the TEM technique for determining dislocation onset, even though TEM is not the most sensitive technique, however; it illustrates, as did the TEM technique, a plan-view of the dislocations and that the theoretical CLT of GaP on GaAs has been exceeded.

The degradation of electrical properties for a fabricated GaP/GaAs Schottky diode was employed to determine the onset of misfit dislocations in the GaP layer or defects at the GaP/GaAs interface. The degradation of electrical properties in devices has been previously used to determine CLT's, for example, increase in leakage current for a p-i-n diode utilizing a GaInAs/InP strained layer superlattice¹ or increases in reverse current and ideality factor for Schottky diodes formed from GaInP/InP strained material system¹⁵. In our experiment, samples with GaP thicknesses of 0 Å, 20 Å, 40 Å, 60 Å, 100 Å, and 140 Å were grown to determine the CLT. The breakdown voltage at $I = -280 \mu\text{A}$ and the reverse current at $V = -1\text{V}$ were measured using a Hewlett-Packard 4145B semiconductor parameter analyzer. Figure 3 and 4 show the dependence of the breakdown voltage and the reverse current on the GaP layer thickness. From the figures, degradation of the electrical properties of these Schottky diodes occurs for GaP films thicker than 60 Å. This is in good agreement with the onset of misfit dislocations seen by TEM.

Degradation of optical properties of GaP/GaAs/GaP strained single quantum wells by low temperature photoluminescence (PL) spectroscopy was also used to verify the onset of dislocations at

the interface. Since the presence of dislocations act as nonradiative recombination centers, PL intensity and linewidth degradation has been used before for determining the CLT¹⁶. For these quantum well experiments, a series of GaP/GaAs/GaP strained single quantum wells were grown by ALE at 500 °C directly on a (100) GaAs substrate. The thicknesses of the GaP barrier layers (20 Å, 40 Å, 60 Å, 80 Å, 120 Å, and 150 Å) were varied while the GaAs well width was held constant at 40 Å. All layer thicknesses were verified with cross-section transmission electron microscopy. A very uniform, two-dimension ALE growth of both GaP and GaAs with abrupt interfaces can be seen in Figure 5, a cross-sectional TEM micrograph of a GaP/GaAs/GaP strained single quantum well grown on a (100) GaAs substrate with barrier and well thicknesses of 60 Å. A plot of the relative PL intensities and the FWHM measured at 22 K (Figure 6) indicates an increase in FWHM in samples with GaP thicknesses in the range and greater than 80 to 120 Å. Similarly, a maximum in relative PL intensity at barrier thicknesses of 120 Å can be seen. The lower PL intensity for barrier layers less than 120 Å is due to reduced quantum confinement; while the increase in FWHM and the associated decrease in intensity for GaP layers greater than 120 Å is due to defect generation at the interfaces. This degradation range (80-120 Å) of the PL emissions from GaP/GaAs/GaP quantum wells is slightly greater than the onset of dislocations seen by TEM (60-80 Å). This discrepancy possibly may be due to strain sharing in the thin GaAs quantum well layer, thereby, increasing the experimentally measured CLT, or it may

simply be a less sensitive detection method.

Experimental CLT values greater than the predicted theoretical CLT values imply that the CLT depends not only on the amount of strain magnitude but on the mode of growth and the growth temperature. Important modes of growth are the three-dimensional (3-D) cluster formation or island growth and the two-dimensional (2-D) Frank-van der Merwe (FM) mode where the film covers the substrate and thickens uniformly. The FM mode is supported for growth temperatures below a certain roughening transition temperature (TR)¹⁷. For thin overlayers the epitaxial strained film is coherent and the mismatch is completely accommodated by elastic strain. As the value of the equilibrium critical thickness is exceeded, it becomes energetically favorable for dislocations to start to appear at the strained interfaces. Therefore, the mismatch will be accommodated by a combination of elastic strain and interfacial misfit dislocations, rather than by elastic strain alone. This behavior is associated with kinetic barriers to the formation and motion of misfit dislocations. Therefore, it is currently believed that during this initial relaxation behavior, if the growth follows a 2D mode, dislocation sources are originated either from substrate threading dislocations^{18,12} or by heterogenous nucleation.^{19,20} The heterogenous nucleation center can be due to small clusters of impurity atoms, localized structural surface defects, or other sources that can produce localized stress concentration. These surface defects can play a major role in the initial stages of relaxation of strained-layer structures, and

their suppression can lead to the retardation of this relaxation process; thus, higher strain can be sustained for a given layer thickness. Therefore, ALE can yield high quality interfaces free from many defects and heterogeneous nucleation centers that can exist in other conventional growth technologies; thereby, higher CLT's can be achieved. Two-dimensional growth is supported by ALE due to the one layer per cycle process where deposition of organometallic group III molecules migrate to their proper lattice sites followed by a reaction with group V hydride for growth of III-V compounds. In this manner, stoichiometric growth is achieved, thus reducing anti-site defects.

Growth at low temperatures is also desirable for maintaining high CLT's. Research of InGaAs films with $x=0.33$ on GaAs substrates²¹ reports the onset of interfacial dislocations and 3D island growth for higher growth temperatures. Therefore, 3D growth is thermodynamically favored in lattice mismatch systems grown at high temperature which can lead to heterogeneous nucleation sites. Furthermore, in a recent publication, InGaAs with In as high as 45% was grown on GaAs well above the CLT at low substrate temperatures⁹. The high CLT's obtained in our results can also be contributed to low temperature growth (500°C) of GaP and ALE 2-D stoichiometric growth.

A potential application of the growth of thick GaP on GaAs is its use as a substitute for AlGaAs in high electron mobility transistors (HEMT's) where the thickness of the AlGaAs layer is used for threshold voltage control²². From preliminary results, we

have found that the etch rate of the ALE grown GaP layers is more than 50 times slower than that of GaAs for H_3PO_4 -based and NH_4OH -based etchants. Even though AlGaAs has a high etching selectivity ratio to GaAs²³, the results suggest that GaP could be a suitable replacement for AlGaAs as an effective stop-etch layer. Furthermore, due to the high surface states of GaAs, passivation of GaAs with a wide-bandgap material lowers the surface recombination velocity²⁴. It has been reported that the interface between phosphorus compounds and GaAs has a lower recombination velocity than the AlGaAs/GaAs interface^{25,26}. The gate Schottky barrier is also increased by the wide-bandgap material. Thus, GaP potentially could be used as an effective stop-etch, passivating layer and increase the Schottky barrier height in metal semiconductor field effect transistor (MESFET) structures.

Conclusion

Highly strained GaP films and GaP/GaAs/GaP single quantum wells were grown on (100) GaAs by low temperature atomic layer epitaxy with GaP layer thicknesses exceeding the theoretical CLT. All characterization techniques confirmed a CLT greater than 60 Å. This high value suggest that the onset of misfit dislocations in the GaP layer can be impeded due to low temperature 2-D ALE growth.

This work is supported by NSF, ONR, SDIO, and NTT.

References

1. H. Tempkin, D.G. Gershon, S.N.G. Chu, J.M. Vandenberg, R.A. Hamm, and M.B. Panish, *Appl. Phys. Lett.* **55**, 1668 (1989).
2. Munecazu Tacano, Yoshinobu Sugiyama, and Yukihiro Takeuchi, *Appl. Phys. Lett.* **58**, 2420 (1991).
3. R. People and J.C. Bean, *Appl. Phys. Lett.* **47**, 322 (1985).
4. D.C. Houghton, D.D. Perovic, J.M. Baribeau, and G.C. Weatherly, *J. Appl. Phys.* **67**, 1850 (1990).
5. W.D. Laidig, C.K. Peng, and Y.F. Lin, *J. Vac Sci. Technol.* **B2**, 181 (1984).
6. I.J. Fritz, S.T. Picraux, L.R. Dawson, T.J. Drummond, W.D. Laidig and N.G. Anderson, *Appl. Phys. Lett.* **46**, 967 (1985).
7. I.J. Fritz, P.L. Gourley, and L.R. Dawson, *Appl. Phys. Lett.* **51**, 1004 (1987).
8. N.G. Anderson, W.D. Laidig, R.M. Kolbas, and Y.C. Lo, *J. Appl. Phys.* **60**, 7 (1986).
9. B. Elman, Emil S. Koteles, P. Melman, K. Ostreicher, and C. Sung, *J. Appl. Phys.* **70**, 2634 (1991).
10. G.C. Osbourn, R.M. Biefeld and P.L. Gourley, *Appl. Phys. Lett.* **41**, 172 (1982).
11. G.C. Osbourn, *J. Appl. Phys.* **53**, 1586 (1982).
12. J.W. Matthews and A.E. Blakeslee, *J. Cryst. Growth* **27**, 118 (1974).
13. J.H. van der Merwe, *CRC Crit. Rev. Solid State Mater. Sci.* **7**, 209 (1978).
14. M.A. Tischler and S.M. Bedair in *Atomic Layer Epitaxy*, edited by T. Suntola and M. Simpson (Blackie, Glasgow and London, 1990), Chap. 4.
15. S. Loualiche, A. Ginudi, A. LeCorre, D. Lecrosnier, C. Vaudry, L. Henry, and C. Guillemot, *Appl. Phys. Lett.* **55**, 2099 (1989).
16. T.G. Anderson, Z.G. Chen, V.D. Kulakovskii, A. Voldin, and J.T. Vallin, *Appl. Phys. Lett.* **51**, 752 (1987).

17. G.H. Gilmer and M.H. Grabow, *Journal of Metals* **June**, 19 (1987).
18. J.W. Matthews, S. Mader, and T.B. Light, *J. Appl. Phys.* **41**, 3800 (1970).
19. Brian W. Dodson, *Appl. Phys Lett.* **53**, 394 (1988).
20. E.A. Fitzgerald, G.P. Watson, R.E. Proano, D.G. Ast, P.D. Kirchner, G.D. Pettit, and J.M. Woodall, *J. Appl. Phys.* **65**, 2220, (1989).
21. G.J. Whaley and P.I. Cohen, *J. Vac. Sci. Technol.* **B6**, 525 (1988).
22. M. Abe, T. Mimura, K. Nishiuchi, A. Shibatomi, and M. Kobayashi, *IEEE J. Quantum Electronics* **22**, 1870 (1986).
23. K. Hikosaka, T. Mimura, and K. Joshin, *Jpn. J. Appl. Phys.* **20**, 1847 (1981).
24. F. Capasso and G.F. Williams, *J. Electrochem. Soc.* **129**, 821 (1982).
25. J.M. Olson, R.K. Ahrenkiel, D.J. Dunlavy, B. Keyes, and A.E. Kibbler, *Appl. Phys. Lett.* **55**, 1208 (1989).
26. Fumiaki Hyuga, Tatsuo Aoki, Suehiro Sugitani, Kazuyoshi Asai, and Yoshihiro Imamura, *MRS Conference* **Fall** (1991).

Figure Captions

- Figure 1. Plan-View TEM Micrographs of GaP Layers Grown On (100) GaAs. (a) 60 Å GaP layer, (b) 80 Å GaP layer, (c) 200 Å GaP layer.
- Figure 2. Chemical Etch Delineation of Dislocations in GaP layer. (a) Mesa Etch of 60 Å GaP Grown on GaAs, (b) Mesa Etch of 140 Å GaP Grown on GaAs
- Figure 3. GaP/GaAs Schottky Diode Breakdown Voltage measured at $I = -280 \mu\text{A}$ for different GaP Thicknesses.
- Figure 4. GaP/GaAs Schottky Diode Reverse Current Measured at $V = -1\text{V}$ for different GaP Thicknesses.
- Figure 5. A Cross-Sectional TEM Micrograph of a 60 Å GaP/ 60 Å GaAs/ 60 Å GaP Strain Quantum Well Grown on (100) GaAs Substrate.
- Figure 6. PL Intensity and FWHM for a GaP/GaAs/GaP SQW's with a Constant GaAs Well Thickness of 40 Å and Various GaP Barrier Thicknesses.

Plan-View TEM Micrographs of GaP Layers Grown On (100) GaAs

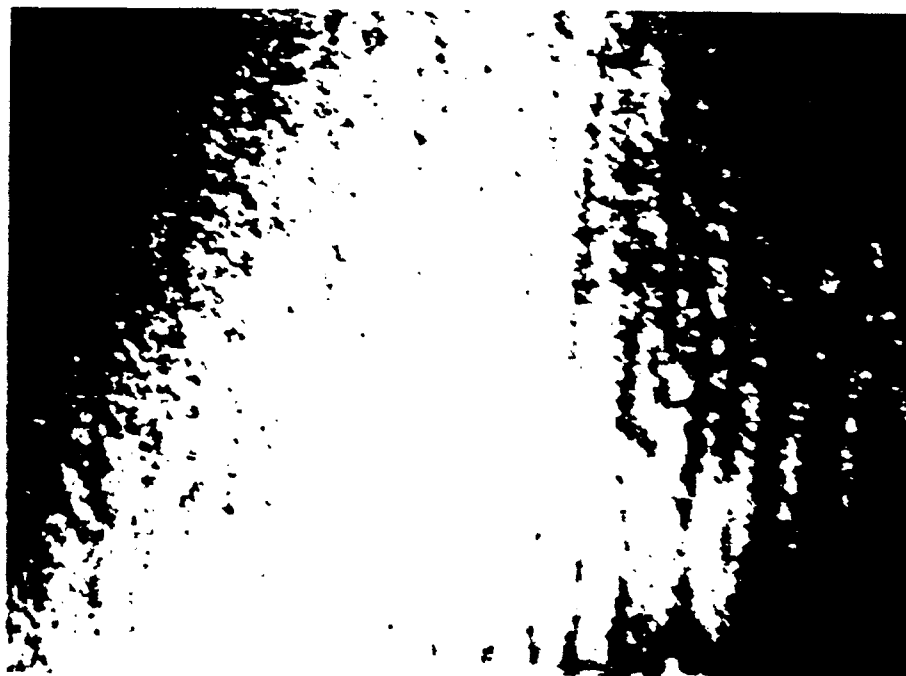


Figure 1(a) 60 Å GaP layer

Plan-View TEM Micrographs of GaP Layers Grown On (100) GaAs



Figure 1(b) 80 Å GaP layer

Plan-View TEM Micrographs of GaP Layers Grown On (100) GaAs

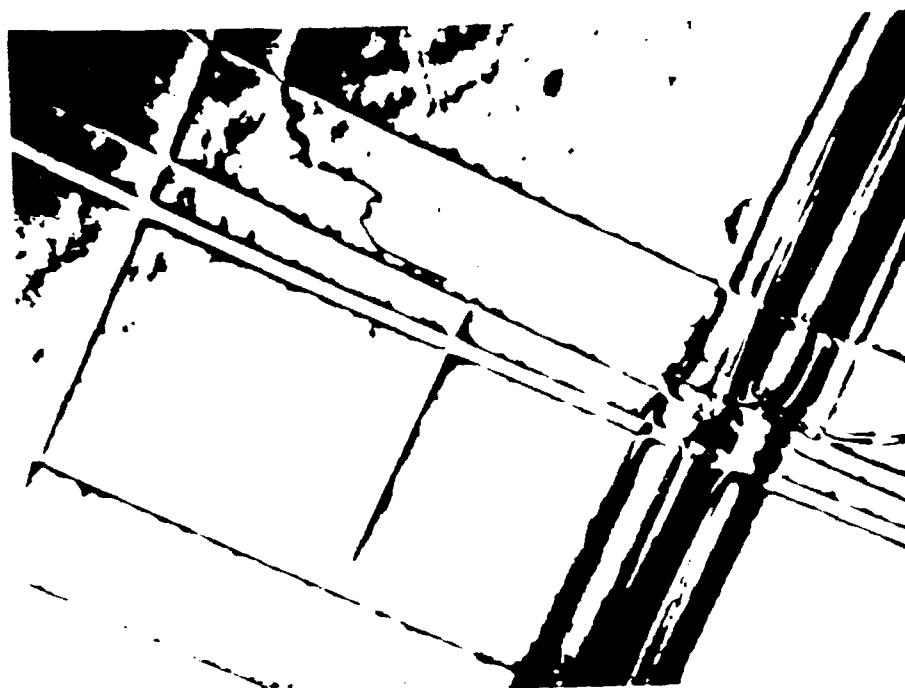


Figure 1(c) 200 Å GaP layer

Chemical Etch Delineation of Dislocations
Formed in the GaP Layer



Figure 2(a). 60 Å GaP grown on GaAs after Mesa Etch

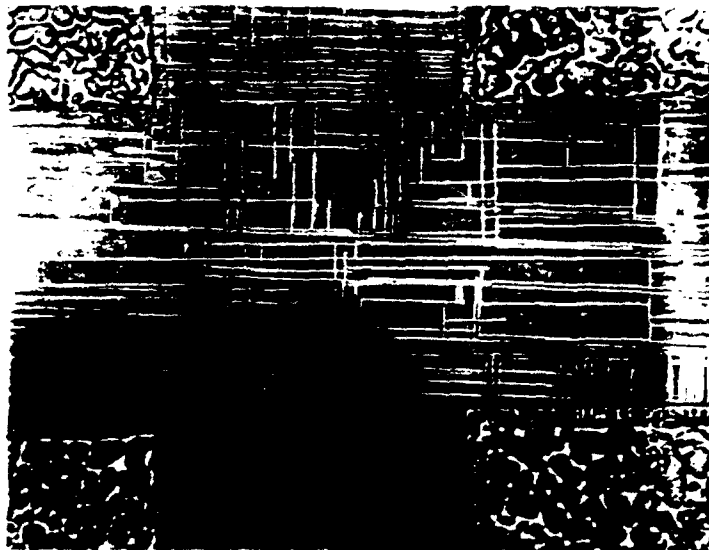


Figure 2(b). 140 Å GaP grown on GaAs after Mesa Etch

GaP/GaAs Schottky Diode Characteristics

Ti/Au Schottky (280um x 280um)

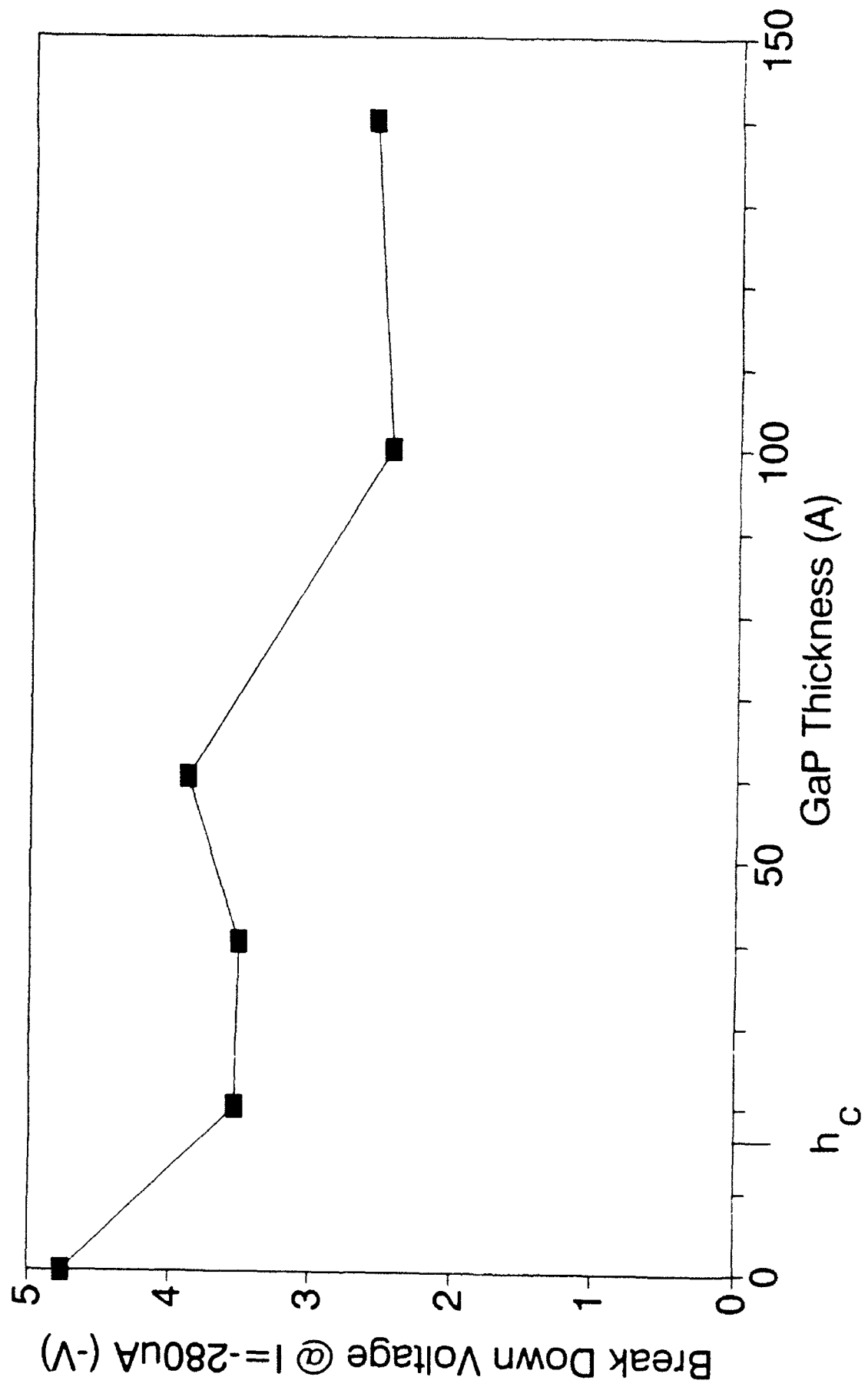


FIGURE 3

GaP/GaAs Schottky Diode Characteristics

Ti/Au Schottky (280um x 280um)

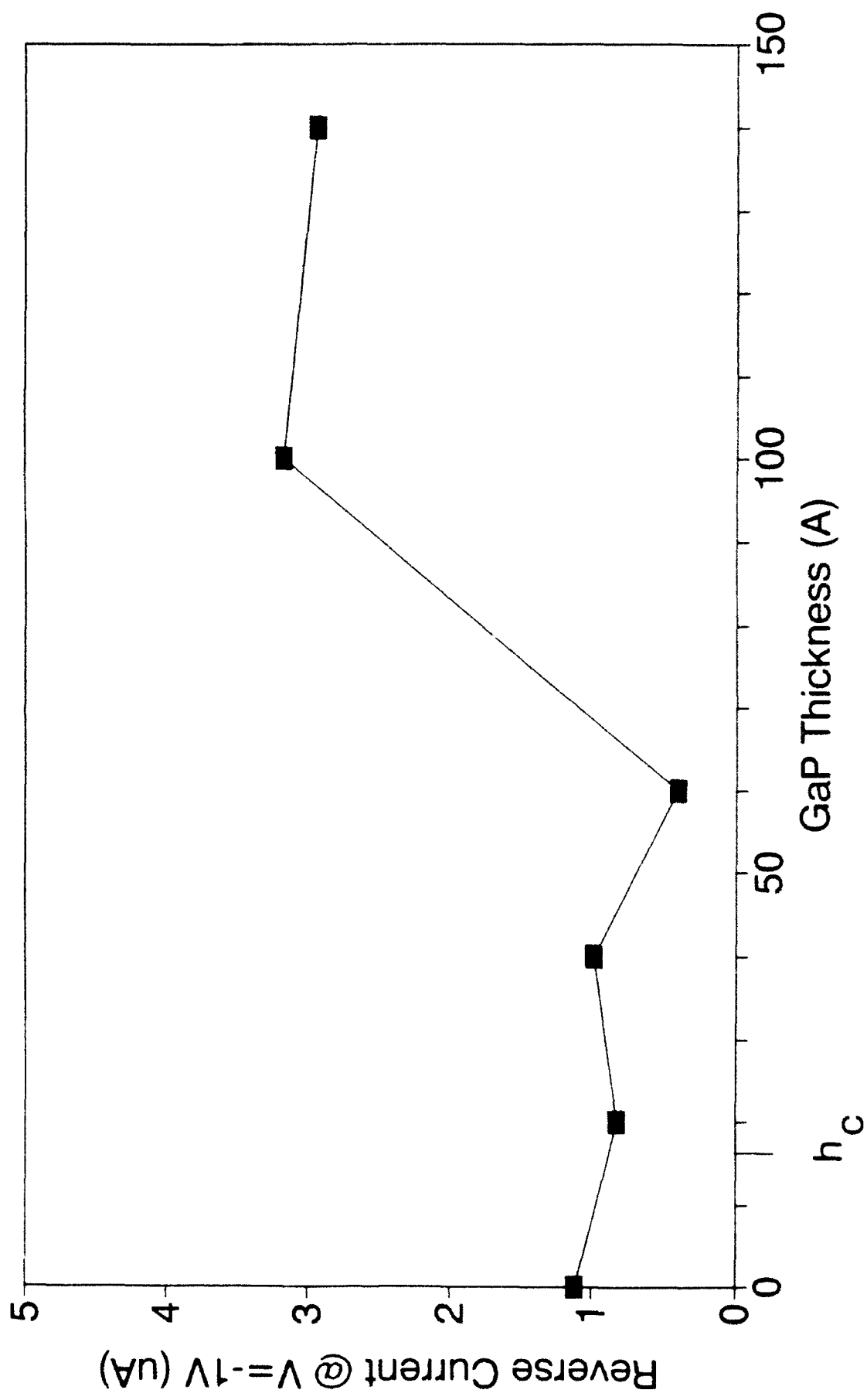


FIGURE 4

A Cross-Sectional TEM Micrograph of a GaP/GaAs/GaP
Strained Quantum Well Grown on (100) GaAs Substrate

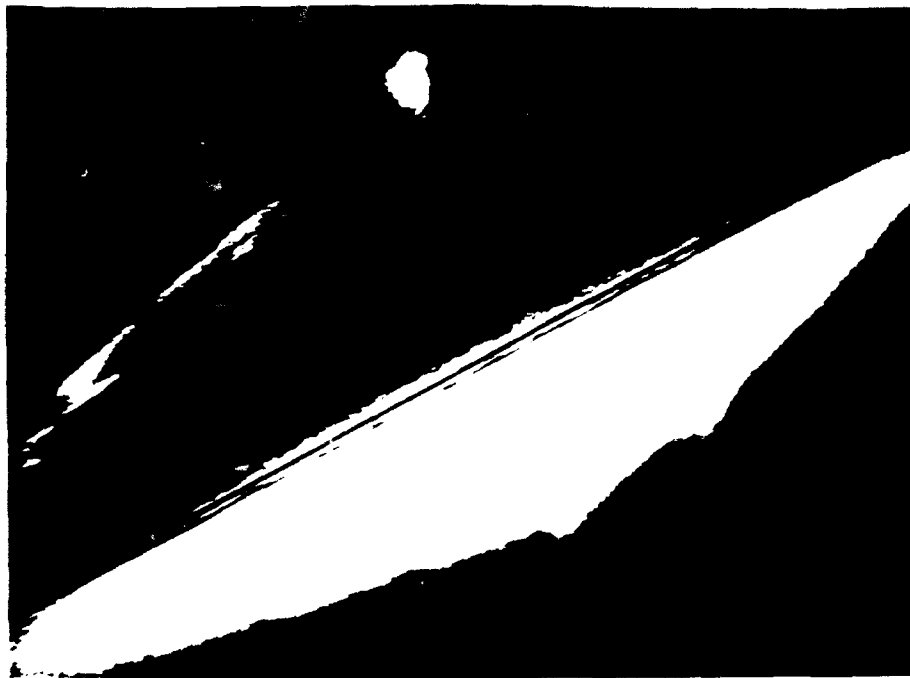


Figure 5. 60 Å GaP/ 60 Å GaAs/ 60 Å GaP SQW

PL Data of GaP/GaAs SQW

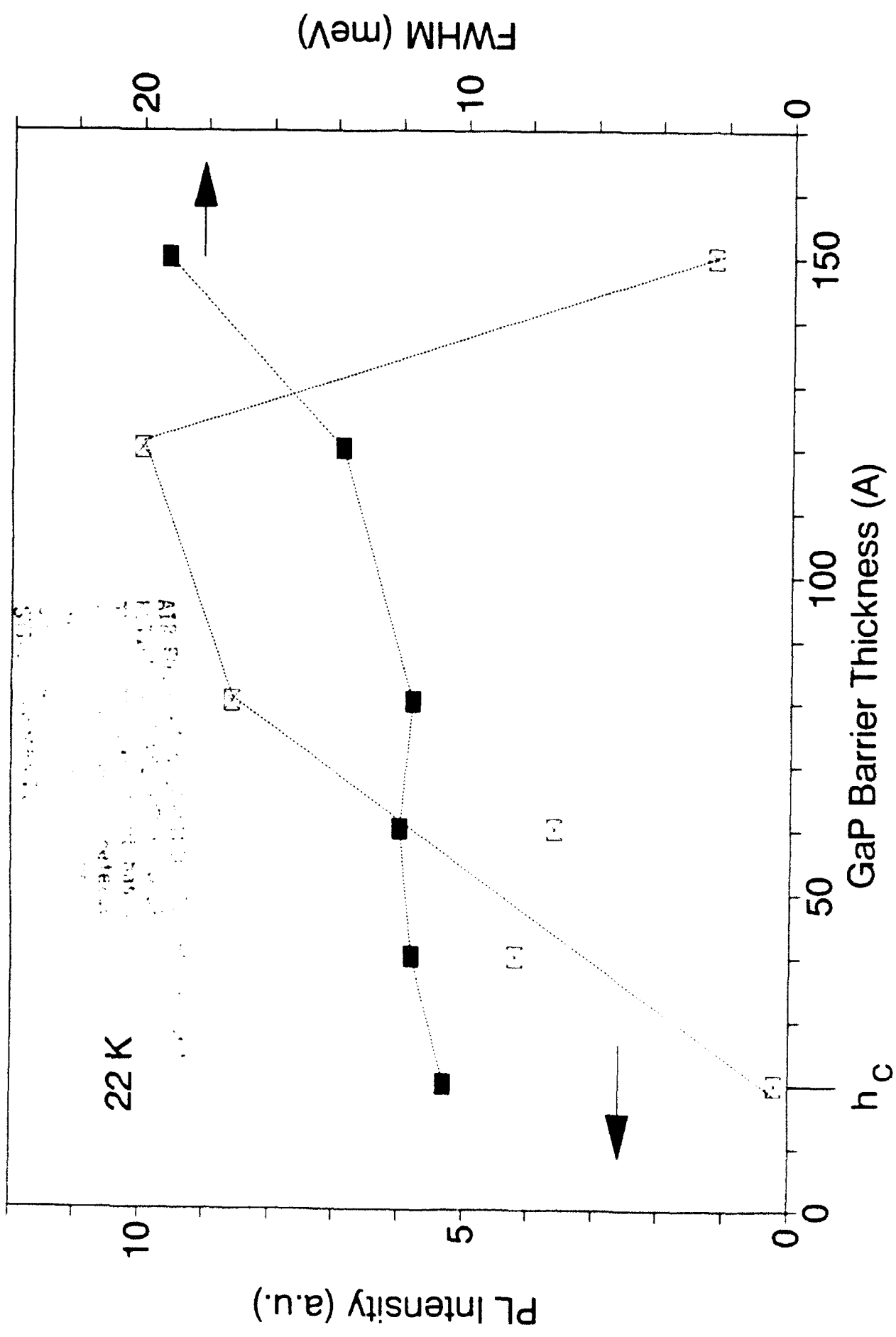


FIGURE 6